Design an Airfoil for a Horizontal Axis Wind Turbine operating at Re=400,000

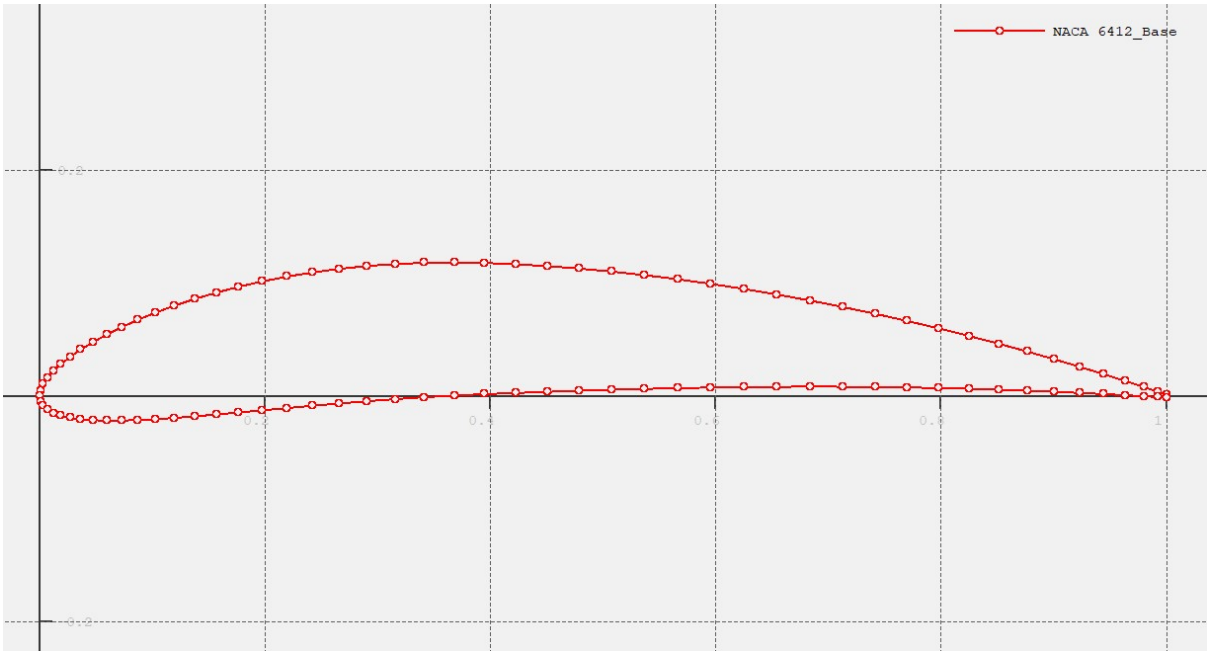

No.	Name	ID	Email
01	Ayman Khan	200108149	ayman.me.200108149@aust.edu
02	Tarek Ahmed	200108144	tarek.me.200108144@aust.edu
03	Nahidul Islam	200108127	nahidul.me.200108127@aust.edu

Contents

List of Tables

List of Figures

Chapter 1

Introduction

1.1 Objectives

The objectives of this research are:

- To design an airfoil for a horizontal axis wind turbine operating at a Reynolds number of 400,000
- To analyze and optimize the airfoil's performance characteristics for this specific application
- To improve upon the base airfoil design to enhance efficiency and power output
- To evaluate the designed airfoil's lift, drag, and moment coefficients
- To assess the airfoil's performance across a range of angles of attack relevant to wind turbine operation

1.2 Base Airfoil

The selection of an appropriate base airfoil is a critical first step in the design process for wind turbine blades. It provides a starting point for optimization and sets the foundation for the aerodynamic performance of the final design. In this section, we discuss our chosen base airfoil and its relevance to our design objectives.

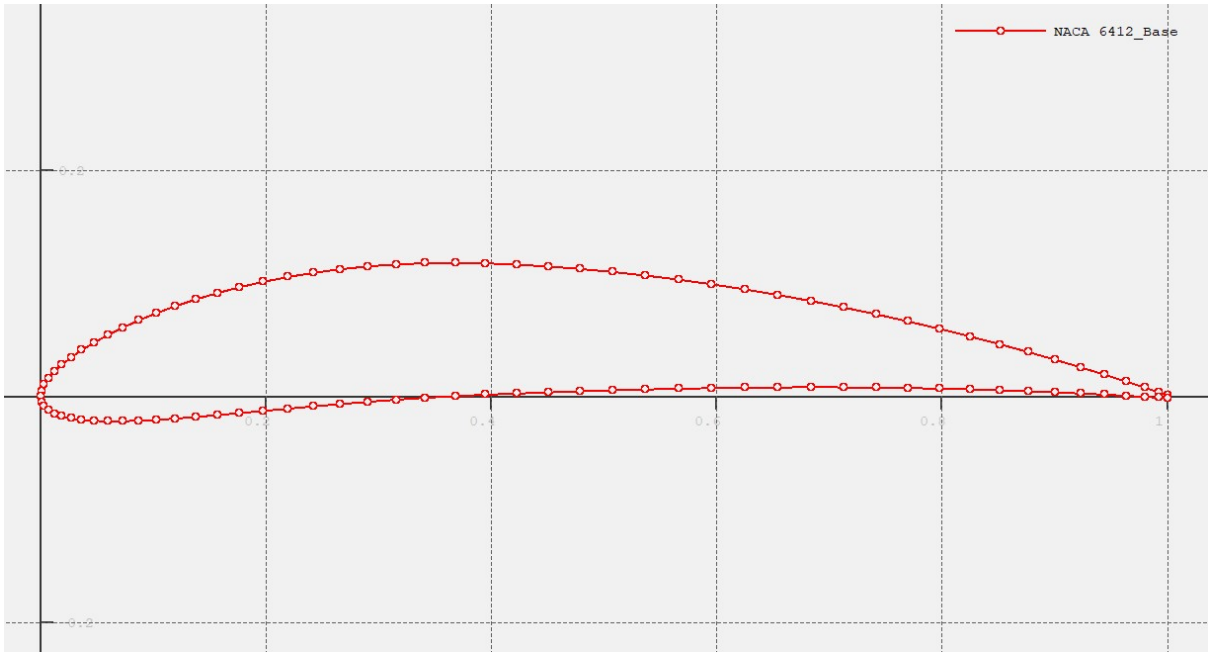

Figure 1.1: NACA 6412 airfoil

For this study, we have selected the NACA 6412 airfoil as our base design. This choice was made to explore and potentially improve upon a known airfoil for horizontal axis wind turbine applications, rather than through a rigorous comparative study.

Key characteristics of NACA 6412:

- Part of the NACA four-digit series
- Maximum camber: 6% at 40% chord from the leading edge
- Maximum thickness: 12% of the chord

These features suggest a potential for good lift-to-drag ratios at our target Reynolds number of 400,000, which is typical for small to medium-sized wind turbines [1].

Our analysis and subsequent modifications will focus on an optimization process that will involve a comprehensive examination of several critical aerodynamic characteristics. Lift generation will be carefully considered, to maximize the airfoil's lift coefficient across operational angles of attack. Simultaneously, drag reduction strategies will be concentrated upon. The airfoil's drag polar will be scrutinized, and the laminar-to-turbulent transition point on the airfoil surface will be managed as part of this process.

Stall characteristics and moment coefficients will also be crucial aspects of our analysis. We'll investigate the airfoil's behavior near and post-stall conditions, aiming to maintain lift and controllability while ensuring stable and efficient rotor dynamics. Throughout this process, we will balance these aerodynamic factors with practical considerations such as structural requirements and manufacturability. Our goal is to develop an optimized design that is both aerodynamically superior and feasible for real-world application in horizontal-axis wind turbines.

1.3 Resources

This section outlines the computational tools and hardware used in our design process. This information is crucial as it defines the capabilities and limitations of our analysis, ensuring reproducibility and providing context for our results.

Our computational setup consists of a system with an AMD Ryzen 5000 series CPU, an NVIDIA GeForce RTX 3060 GPU with 6GB VRAM, and 16GB of RAM, running on Windows 11. The primary design analysis tool for this study is XFLR5, an open-source software for airfoil analysis and design.

This hardware configuration is well-suited for running XFLR5 without any performance issues. The AMD Ryzen 5000 series CPU provides excellent single-core and multi-core performance, beneficial for the computational tasks in XFLR5. The 16GB of RAM is sufficient for handling the memory requirements of airfoil analysis and design tasks. XFLR5 runs smoothly on Windows 11, with no compatibility issues observed. The software's computational demands are well within the capabilities of our hardware, allowing for quick iterations and real-time visualization of results.

While XFLR5 is our primary tool, it's important to consider the potential for more advanced Computational Fluid Dynamics (CFD) analyses using software like ANSYS Fluent. In this context, our setup provides a solid foundation but may require some enhancements for extensive CFD work. The CPU is capable of handling complex CFD simulations, although computation times may be significant for highly detailed models. The NVIDIA GeForce RTX 3060 GPU with 6GB VRAM is suitable for accelerating certain CFD calculations, particularly in ANSYS Fluent which supports GPU acceleration.

However, the 6GB VRAM may become a limiting factor for very large or complex simulations.

Key considerations for potential CFD work include:

- The 16GB of system RAM is adequate for moderate CFD simulations but may need to be upgraded for more demanding cases.
- For extensive CFD work, a GPU with more VRAM would be beneficial.
- While Windows 11 is fully compatible with both XFLR5 and ANSYS Fluent, some researchers prefer Linux-based systems for CFD work. Our Windows 11 setup does not preclude the use of these tools, as we can utilize Windows Subsystem for Linux (WSL) if needed.

Our current setup is more than capable of our primary analysis using XFLR5. It also provides a solid foundation for potential future work with more advanced CFD tools, although some upgrades might be beneficial for extensive CFD simulations.

Throughout this study, we will leverage these resources to conduct detailed aerodynamic analyses, perform parametric studies, and evaluate the performance of our airfoil designs under specified operating conditions. The results obtained from these analyses will guide our design decisions and inform the development of an optimized airfoil for the target application.

Chapter 2

Literature Review

Horizontal Axis Wind Turbines (HAWT) are widely regarded as one of the most efficient designs for wind energy conversion. The turbine blades, rotating around a horizontal axis, extract energy from the wind, converting kinetic energy into mechanical power. This design dominates the wind energy sector, primarily due to its ability to operate efficiently across various wind speeds and its maturity in commercial and utility-scale projects.

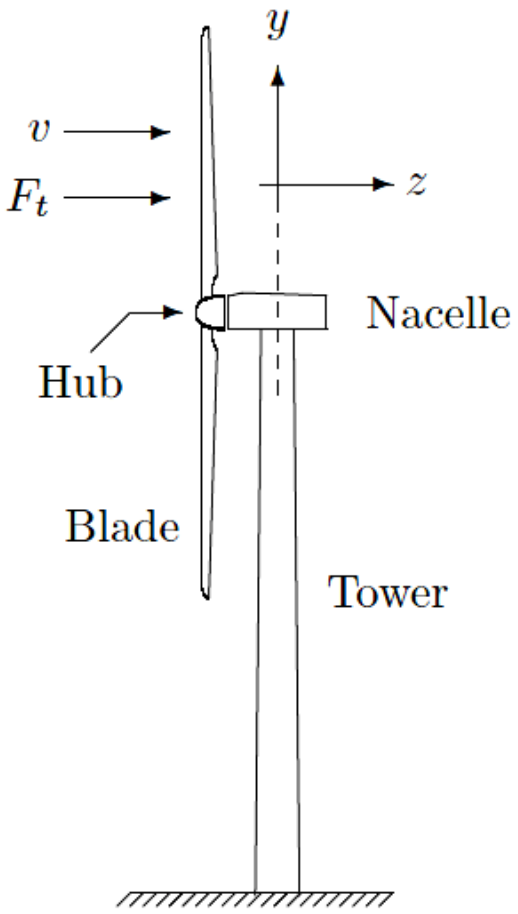

Figure 2.1: Schematics of Horizontal Axis Wind Turbine (HAWT)

Several researchers have examined the advantages of HAWTs over other wind turbine designs, such as Vertical Axis Wind Turbines (VAWT). Burton et al. (2011), in their seminal work on wind energy systems, emphasized that HAWTs offer higher efficiency, particularly in high-wind environments, due to their larger rotor diameter and the ability to harness a greater swept area [2]. Manwell et al. (2010) also supported this, stating that HAWTs achieve higher capacity factors and better performance-to-cost ratios compared to their vertical-axis counterparts [3]. The performance of HAWT blades is highly dependent on the aerodynamic properties of the airfoil used. The design of the airfoil influences the lift and drag

forces generated as wind flows over the blade. Sørensen (2011) highlighted that optimizing airfoil shape can significantly improve energy extraction, especially at low Reynolds numbers where laminar-turbulent transition plays a critical role [4]. This project will use NACA 6412 as our base airfoil, which is a well-studied airfoil for low-Reynolds-number flows, as the foundation for further optimization.

2.1 Fundamental Equations

The design and analysis of airfoils for a Horizontal Axis Wind Turbine (HAWT) operating at a Reynolds number of 400,000 rely on several fundamental aerodynamic equations. These equations help to understand the fluid dynamics around the airfoil and are used in computational tools such as XFLR5 to predict performance.

Continuity Equation

The continuity equation ensures the conservation of mass in an incompressible fluid flow. It is written as:

$$\nabla \cdot \mathbf{V} = 0 \tag{2.1}$$

In the context of airfoil design for a HAWT, this equation ensures that the air moving over the airfoil remains continuous, without any loss or gain of mass in the control volume. At a Reynolds number of 400,000, which corresponds to low-speed, incompressible flow, maintaining mass conservation is essential for predicting airflow over the blade's surface.

Navier-Stokes Equations

The Navier-Stokes equations describe the conservation of momentum in fluid flow, accounting for both inertial and viscous forces. For incompressible flow, they are expressed as:

$$\rho \left(\frac{\partial \mathbf{V}}{\partial t} + \mathbf{V} \cdot \nabla \mathbf{V} \right) = -\nabla P + \mu \nabla^2 \mathbf{V} \tag{2.2}$$

For airfoil design at a Reynolds number of 400,000, the Navier-Stokes equations are crucial because they help predict the balance between inertial forces (which dominate at higher speeds) and viscous forces (which dominate at lower speeds). At this Reynolds number, the flow is typically in the transition range between laminar and turbulent, and the viscous effects captured by these equations are vital for predicting drag and boundary layer behavior.

Bernoulli's Principle

Bernoulli's equation describes the conservation of mechanical energy in a steady, incompressible flow. It is given by:

$$P + \frac{1}{2}\rho V^2 + \rho g h = \text{constant} \tag{2.3}$$

When designing an airfoil for HAWT, Bernoulli's principle explains how pressure differences across the airfoil generate lift. At a Reynolds number of 400,000, the airflow velocity is relatively moderate, and the pressure differential between the upper and lower surfaces of the airfoil must be optimized to maximize lift without inducing excessive drag.

Lift and Drag Coefficients

The lift and drag coefficients quantify the non-dimensional forces acting on the airfoil. They are defined as:

$$C_L = \frac{L}{\frac{1}{2}\rho V^2 A}, \quad C_D = \frac{D}{\frac{1}{2}\rho V^2 A} \tag{2.4}$$

In designing a HAWT airfoil at a Reynolds number of 400,000, the lift coefficient C_L and drag coefficient C_D are key performance indicators. At this Reynolds number, we seek an airfoil that maximizes C_L to generate sufficient lift while minimizing C_D to reduce drag, enhancing the turbine's efficiency in converting wind energy to mechanical power.

Reynolds Number

The Reynolds number Re is a dimensionless quantity that determines the flow regime—whether it is laminar or turbulent. It is given by:

$$Re = \frac{\rho V c}{\mu} \tag{2.5}$$

At a Reynolds number of 400,000, the flow is in the transitional region between laminar and turbulent. This affects both the lift and drag characteristics of the airfoil. For HAWT airfoils, optimizing performance in this range requires careful balancing of aerodynamic shape to ensure favorable boundary layer development and minimize drag while maintaining lift.

Moment Coefficient

The moment coefficient C_M describes the pitching moment on the airfoil, which influences its stability and control. It is defined as:

$$C_M = \frac{M}{\frac{1}{2}\rho V^2 c} \tag{2.6}$$

In the design of airfoils for wind turbines, especially at high Reynolds numbers around 400,000, the moment coefficient C_M helps ensure that the airfoil does not experience large, undesirable moments that could destabilize the turbine blades. A well-balanced moment coefficient contributes to the stability of the turbine during operation.

Lift-to-Drag Ratio

The lift-to-drag ratio is a key indicator of aerodynamic efficiency and is written as:

$$\frac{C_L}{C_D} \tag{2.7}$$

For a HAWT operating at a Reynolds number of 400,000, achieving a high lift-to-drag ratio is essential for efficient energy extraction. A high ratio means that the airfoil generates significant lift with minimal drag, maximizing the turbine's performance, particularly at lower wind speeds.

Application to XFLR5

XFLR5 uses these fundamental equations to simulate the aerodynamic behavior of airfoils, providing key performance metrics such as lift, drag, and moment coefficients. At a Reynolds number of 400,000, the following performance plots will be generated during the computational analysis of the NACA 6412 airfoil:

- C_L vs. α: Lift coefficient as a function of angle of attack.
- C_D vs. α: Drag coefficient as a function of angle of attack.
- C_L/C_D vs. α: Lift-to-drag ratio as a function of angle of attack.
- C_M vs. α: Moment coefficient as a function of angle of attack.
- C_L vs. C_D: Drag Polar.

These results will provide a comprehensive assessment of the airfoil's suitability for HAWT applications at the chosen Reynolds number.

2.2 Computational Aerodynamic Tool(s)

For the aerodynamic analysis of the NACA 6412 airfoil, we will use *XFLR5*, a widely accepted tool for low-Reynolds-number airfoil design. XFLR5 combines potential flow theory with boundary layer analysis, allowing for accurate predictions of airfoil performance in both laminar and turbulent flow regimes.

Several researchers have validated XFLR5's accuracy in low-Reynolds-number applications. Hamid et al (2022) demonstrated its effectiveness in analyzing airfoils for micro aerial vehicles, which operate under similar Reynolds number conditions to HAWTs [5]. Le et al (2023) also confirmed that XFLR5 produces results consistent with experimental wind tunnel data for small wind turbine airfoils [6].

XFLR5 has been used in various other studies to evaluate airfoil performance in renewable energy systems. used XFLR5 to investigate airfoils for small wind turbines, demonstrating that the software provides reliable lift, drag, and moment predictions when compared with experimental data [7]. The aerodynamic graphs generated by XFLR5 will be compared against experimental data to validate the tool's accuracy, particularly at the Reynolds number range of interest.

2.3 Experimental Data for Validation

Validation is a critical component of aerodynamic research, ensuring that computational models reflect real-world behavior. For this project, we will validate our XFLR5 results using data from the catalog of low-Reynolds number airfoil data for wind-turbine applications [8]. Miley's work offers comprehensive experimental data on various airfoils tested under low-Reynolds-number conditions, including lift, drag, and moment coefficients.

In addition to Miley's data, other experimental studies will provide further validation. Selig et al. (1995) [9] conducted wind tunnel tests on several airfoils at low Reynolds numbers, offering a valuable benchmark for comparing our XFLR5 predictions. Somers et al (1997) [10] also provides detailed experimental data on airfoils designed specifically for wind turbine applications, further ensuring the robustness of our validation process.

Zhang et al [11] reveals that for airflow and turbulence in enclosed environments, deviations of less than 10% between CFD predictions and experimental data are considered indicative of good model performance. Meanwhile, deviations of less than 20% are regarded as acceptable. This assessment provides a clear standard for gauging the reliability of analysis tools for CFD in confined settings, ensuring that models remain within a reasonable margin of error when compared to empirical observations.

Chapter 3

Validation Analysis

In this chapter, the primary goal is to validate the simulated aerodynamic performance data generated using XFLR5 with experimental data from Miley's catalog. This involves validating the lift coefficient (CL) and drag coefficient (CD) before going with the design of our selected airfoil to know whether XFLR5 data are reliable or not.

Formulas:

Two important formulas are used for comparing results, one is percent difference (%Diff) and the latter is percent error (%Err). These metrics are crucial for comparing and validating different sets of data, such as simulated results at different Reynolds numbers or simulated results against experimental data.

$$\%\text{Diff} = \frac{V_1 - V_2}{\frac{1}{2}(V_1 + V_2)} \times 100 \tag{3.1}$$

$$\%\text{Err} = \frac{V_c - V_r}{V_r} \times 100 \tag{3.2}$$

Percentage difference (%Diff) quantifies the relative difference between two values (V_1 and V_2), treating both with equal weight. This symmetric comparison is particularly useful when neither value is considered a standard or reference. A positive %Diff indicates that V_1 is greater than V_2, while a negative %Diff signifies the opposite. This metric proves valuable when comparing two sets of data, such as comparing simulation results at different conditions, evaluating the impact of design modifications, or contrasting experimental findings. In a validation process, %Diff helps assess the degree of agreement or discrepancy between two sets of results, offering insights into the sensitivity of the analysis to specific parameters or assumptions.

Percentage error (%Err) assesses the deviation of a calculated value (V_c) from a reference value (V_r). This asymmetric metric is appropriate when one value serves as a known standard or benchmark. A positive %Err indicates that V_c overestimates the reference value (V_r), while a negative %Err signifies an underestimation. Percentage error is commonly used to validate simulations against experimental data, assess the accuracy of models, or quantify the uncertainty in measurements. During validation, %Err provides a direct measure of how well the calculated or simulated values align with the established reference, indicating the level of confidence in the predictive capabilities of a model or the reliability of experimental measurements.

By analyzing the trends in %Diff and %Err, researchers can identify systematic biases, validate computational models, and ascertain the reliability of simulations under different conditions.

3.0.1 Feasibility of Using RN = 400,000 for Validation

Before performing the validation, we need to determine whether the simulated results at RN = 400,000 can be compared with the experimental values at RN = 330,000. To do this, we compare the simulated results for CL and CD at both RN = 330,000 and RN = 400,000 which is provided in table 3.1. Here, V_1, and V_c from equation 3.1 and 3.2 will be considered as CL at 400,000 Reynolds number and CD at 400,000 Reynolds number.

Table 3.1: Comparison of Simulated Lift and Drag Coefficients at Different Reynolds Numbers

	Lift Coefficient (CL)				**Drag Coefficient (CD)**			
AOA	**Re = 330,000**	**Re = 400,000**	**%Diff**	**%Err**	**Re = 330,000**	**Re = 400,000**	**%Diff**	**%Err**
-7	-0.07	-0.07	0.94	-0.93	0.0225	0.0182	-21.06	23.53
-6	0.03	0.03	8.05	-7.74	0.0168	0.0146	-14.59	15.74
-5	0.14	0.14	1.72	-1.71	0.0139	0.0129	-7.10	7.36
-4	0.25	0.25	0.52	-0.52	0.0124	0.0116	-7.17	7.44
-3	0.36	0.36	0.39	-0.39	0.0114	0.0106	-7.72	8.03
-2	0.47	0.47	0.32	-0.32	0.0109	0.0102	-6.75	6.99
-1	0.58	0.58	0.19	-0.19	0.0106	0.0100	-6.01	6.20
0	0.69	0.69	0.23	-0.23	0.0106	0.0100	-5.54	5.70
1	0.78	0.79	1.13	-1.12	0.0096	0.0097	0.52	-0.52
2	0.88	0.90	2.34	-2.31	0.0101	0.0098	-3.42	3.48
3	1.00	1.00	0.26	-0.26	0.0107	0.0100	-7.06	7.32
4	1.10	1.11	0.25	-0.25	0.0114	0.0107	-6.78	7.02
5	1.21	1.21	0.14	-0.14	0.0122	0.0115	-5.90	6.08
6	1.31	1.31	0.20	-0.20	0.0132	0.0122	-7.40	7.69
7	1.41	1.41	0.19	-0.19	0.0142	0.0132	-7.25	7.52
8	1.49	1.49	0.11	-0.11	0.0151	0.0142	-6.43	6.64
9	1.55	1.56	0.24	-0.24	0.0164	0.0156	-5.31	5.46
10	1.60	1.60	0.03	-0.03	0.0190	0.0186	-2.39	2.42
11	1.60	1.60	0.41	0.41	0.0250	0.0253	–1.03	-1.03
12	1.58	1.59	0.40	-0.40	0.0349	0.0342	-1.91	1.93
13	1.56	1.58	1.00	-1.00	0.0458	0.0442	-3.65	3.71
14	1.55	1.57	1.22	-1.21	0.0581	0.0559	-3.77	3.85
15	1.54	1.56	1.64	-1.63	0.0722	0.0691	-4.40	4.50
16	1.51	1.55	2.28	-2.26	0.0880	0.0834	-5.31	5.45
17	1.50	1.53	1.87	-1.85	0.1024	0.0987	-3.70	3.77
18	1.49	1.51	0.96	-0.96	0.1173	0.1154	-1.59	1.60
19	1.48	1.50	1.60	-1.58	0.1323	0.1295	-2.10	2.12
20	1.48	1.50	1.10	-1.09	0.1456	0.1441	-1.08	1.09
21	1.48	1.49	0.84	-0.83	0.1601	0.1592	-0.56	0.56

When comparing the simulated lift coefficient (CL) values between RN=330,000 and RN=400,000, the results from table 3.1 indicate that the differences are minimal across a broad range of angles of attack (AOA). The percentage differences between the two sets of values remain small, typically within a margin that does not significantly impact aerodynamic performance. For the majority of the AOA values, the discrepancy is minimal—often less than 2%—suggesting that the airfoil's aerodynamic behavior does not change dramatically between these Reynolds numbers.

For CD, although drag is more sensitive to changes in Reynolds number, the comparison between RN = 330,000 and RN = 400,000 shows that the differences are within acceptable limits, particularly at lower angles of attack, where drag is more critical to performance. At higher angles of attack, where the drag increases due to flow separation and other factors, the differences between the two Reynolds numbers become slightly more pronounced. However, even in these cases, the percentage differences remain

manageable, and the impact on the overall validation process would be minimal.

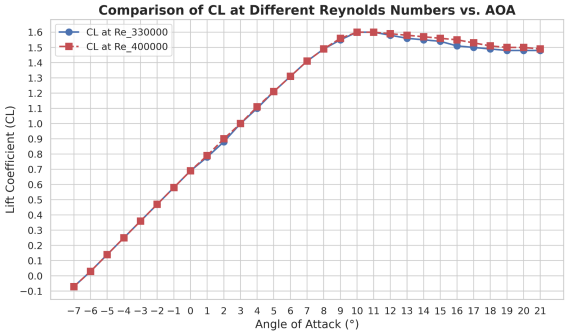

Figure 3.1: Comparison of CL at different RN

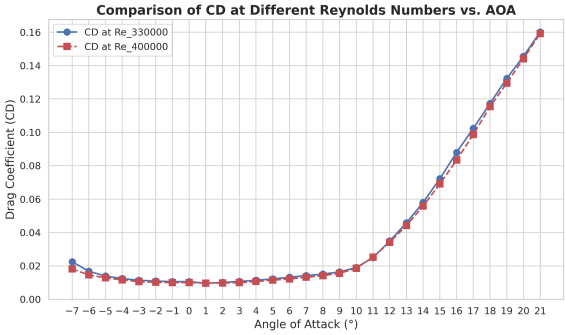

Figure 3.2: Comparison of CD at different RN

Based on this analysis, we can confidently use the simulated values at RN = 400,000 for validation against the experimental data at RN = 330,000. This approach ensures that our validation is closely aligned with our design target and also

3.0.2 Experimental Setup and Simulation Methodology

To validate our simulation results against experimental data, we referenced the catalog by Miley (1982) as the primary validation source. The experimental setup, as detailed in this catalog, was conducted in the NACA Variable Density Tunnel (VDT) in 1937. The test conditions were characterized by three-dimensional flow with a turbulence intensity of 2% and a smooth airfoil surface.

Our objective was to calibrate our simulation parameters to match these experimental conditions closely. To achieve this, we employed XFLR5, a widely used airfoil analysis and design software. A key parameter in XFLR5 that significantly influences the simulation results is the critical amplification ratio, denoted as n_{crit}. This parameter is crucial in the e^n method for transition prediction, which determines the location of laminar-to-turbulent transition on the airfoil surface.

We conducted a series of simulations with varying n_{crit} values which are displayed in Figure 3.3 to identify the setting that best replicates the experimental conditions described in Miley's catalog. The simulations were performed for three different n_{crit} values: 9 (default value in XFLR5), 7, and 5. For each n_{crit} value, we simulated the lift coefficient (C_L) and drag coefficient (C_D) across a range of angles of attack (AOA) from -7° to 21°. These simulated results were then compared against the experimental values provided in Miley's (1982) catalog.

We are trying to determine which n_{crit} value produces simulation results that most closely align with the experimental data. This calibration process is essential for ensuring that our simulations accurately reflect the experimental conditions of the NACA VDT tests. By identifying the optimal n_{crit} value, we can establish a validated baseline for further CFD analyses and initiate the design process of NACA 6412 airfoil for optimization.

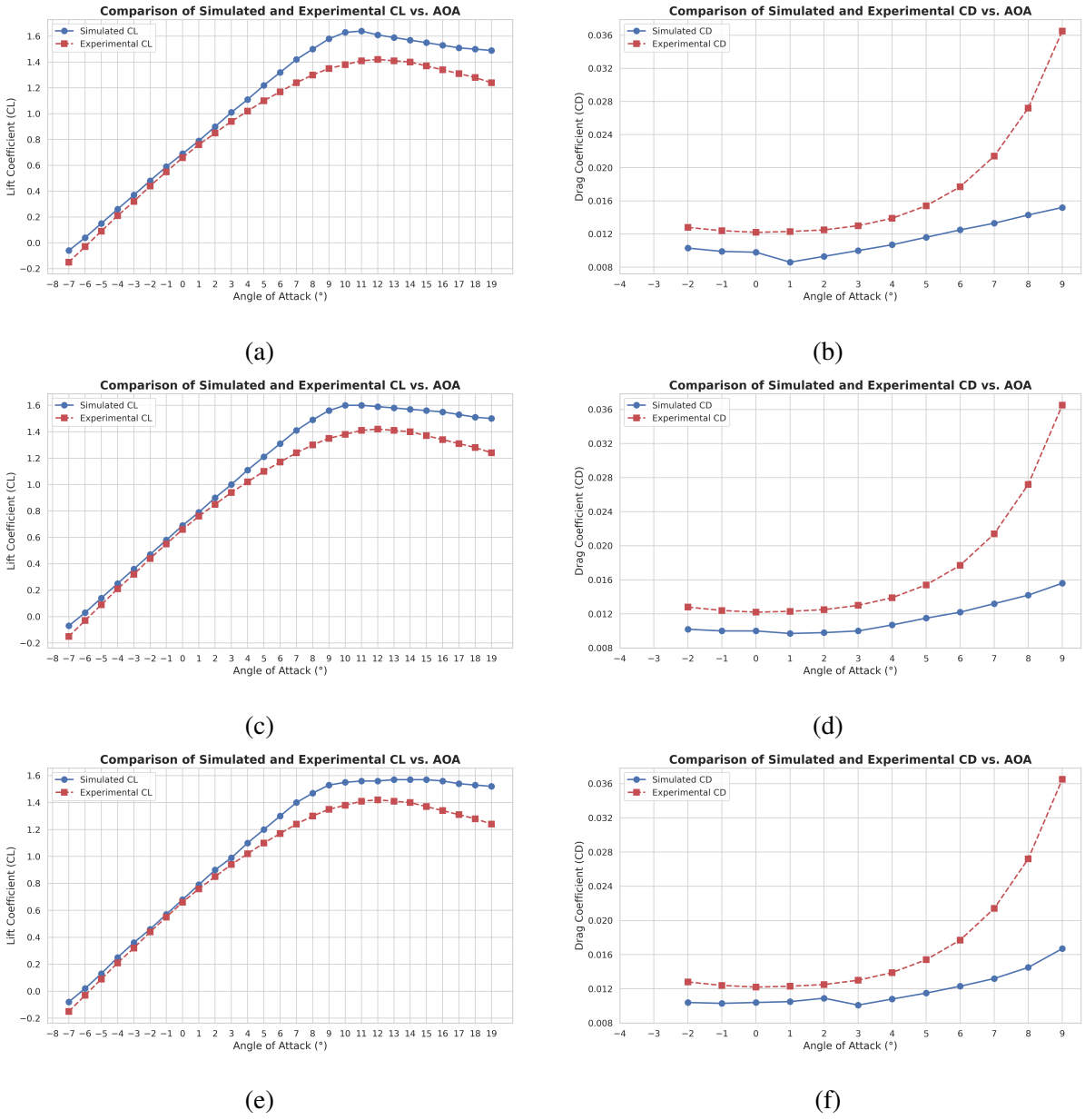

Figure 3.3: Comparison of simulated and experimental CL and CD results against AOA for different nCrit values: (a, b) nCrit = 9, (c, d) nCrit = 7, and (e, f) nCrit = 5

By discerning the graphs provided above, we can easily identify that an n_{crit} value of 7 yielded the closest match to experimental data from the NACA Variable Density Tunnel tests (Miley, 1982). Simulating lift (CL) and drag (CD) coefficients across angles of attack from -7° to 21° with n$crit$ values of 9, 7, and 5, we found that n$crit$ = 7 offered the highest consistency, reflecting the moderate turbulence intensity (2%) reported in the original setup. This calibration enhances the accuracy of our CFD model, aligning it closely with historical data and providing a solid foundation for further aerodynamic analyses.

3.1 Validation of the Lift Coefficients

The validation study presented in Table 3.2 examines the precision of XFLR5's lift coefficient predictions across various angles of attack (AOA). This analysis aims to determine the trustworthiness of XFLR5-generated data for future aerodynamic design projects. Here, V_1, and V_c from equation 3.1 and 3.2 will be considered as simulated CD.

Table 3.2: Simulated and Experimental Lift Coefficient (CL) Comparison

AOA	Sim.	Expe.	%Diff	%Err
-7	-0.07	-0.15	-66.79	-50.07
-6	0.03	-0.03	12200.00	-203.33
-5	0.14	0.09	43.95	56.33
-4	0.25	0.21	17.87	19.62
-3	0.36	0.32	12.23	13.03
-2	0.47	0.44	6.91	7.16
-1	0.58	0.55	5.31	5.45
0	0.69	0.66	4.08	4.17
1	0.79	0.76	4.31	4.41
2	0.90	0.85	5.80	5.98
3	1.00	0.94	6.34	6.54
4	1.11	1.02	8.14	8.49
5	1.21	1.10	9.48	9.95
6	1.31	1.17	11.42	12.11
7	1.41	1.24	12.76	13.63
8	1.49	1.30	13.56	14.55
9	1.56	1.35	14.32	15.42
10	1.60	1.38	14.85	16.04
11	1.60	1.41	12.47	13.30
12	1.59	1.42	10.99	11.63
13	1.58	1.41	11.41	12.10
14	1.57	1.40	11.68	12.40
15	1.56	1.37	13.15	14.08
16	1.55	1.34	14.49	15.63
17	1.53	1.31	15.62	16.94
18	1.51	1.28	16.28	17.73
19	1.50	1.24	19.12	21.14

In chapter 2, we have found that deviations of less than 10% indicate strong model performance, while those below 20% are considered acceptable. We have provided a tabular form of validation analysis for C_L to assess XFLR5's accuracy against these benchmarks. The experimental values are taken from Miley's catalog (1982).

Table 3.3: Validation of Lift Coefficient

AOA Range	%Diff Range	%Err Range	Mean %Diff	Mean %Err	Validation Status
Low(-7° to -5°)	43.95% to 66.79%	50.07% to 56.33%	55.37%	53.20%	Not validated
Moderate(-4° to 11°)	4.08% to 17.87%	4.17% to 19.62%	9.40%	9.74%	Good
High(12° to 19°)	10.99% to 19.12%	11.63% to 21.14%	14.06%	15.11%	Acceptable
Overall	4.08% to 66.79%	4.17% to 56.33%	11.76%	12.85%	Validated for moderate and high AOA

In the low angle of attack (AOA) range, XFLR5 shows significant discrepancies with experimental data, struggling to accurately model flow behavior. This is likely due to complex phenomena such as flow separation or laminar-turbulent transition, making the data unreliable for critical design decisions. However, in the moderate AOA range, XFLR5 closely aligns with experimental results, showing excellent agreement. This range's predictions are sufficiently accurate for most aerodynamic applications, validating its use for design and analysis. At higher AOAs, XFLR5's accuracy slightly decreases, but the

data remains valuable, although caution is advised for critical points.

Considering the overall performance across the entire AOA range from -7° to 19° (excluding the outlier), XFLR5 provides generally reliable lift coefficient predictions, with the best performance in the moderate range. While accuracy drops at the extremes, the tool's predictions align well enough with experimental data to be useful, especially when weighted towards the more accurate moderate AOAs.

3.2 Validation of the Drag Coefficients

The validation analysis for drag coefficient (C_D) predictions, as presented in Table 3.4, indicates varying degrees of accuracy across the angle of attack (AOA) range. This study assesses the reliability of XFLR5's drag predictions for aerodynamic design purposes compared with the data taken from Miley's catalog. Here, V_1, and V_c from equation 3.1 and 3.2 will be considered as simulated CD.

Table 3.4: Simulated and Experimental Drag Coefficient (CD) Comparison

AOA	Sim.	Expe.	%Diff	%Err
-2	0.0102	0.0128	-22.78	-20.45
-1	0.0100	0.0124	-21.48	-19.40
0	0.0100	0.0122	-19.95	-18.14
1	0.0097	0.0123	-23.86	-21.32
2	0.0098	0.0125	-24.72	-22.00
3	0.0100	0.0130	-26.05	-23.05
4	0.0107	0.0139	-25.95	-22.97
5	0.0115	0.0154	-28.55	-24.98
6	0.0122	0.0177	-36.81	-31.09
7	0.0132	0.0214	-47.85	-38.61
8	0.0142	0.0272	-63.10	-47.97
9	0.0156	0.0365	-80.34	-57.32

The validation criteria established in chapter 2 are similarly applied to C_D, and we have provided a table to assess XFLR5's performance accordingly.

Table 3.5: Validation of Drag Coefficient

AOA Range	%Diff Range	%Err Range	Mean %Diff	Mean %Err	Validation Status
Low(-2° to 1°)	19.95% to 23.86%	18.14% to 21.32%	22.02%	19.83%	Acceptable
Moderate(2° to 5°)	24.72% to 28.55%	22.00% to 24.98%	26.32%	23.25%	Acceptable
High(6° to 9°)	36.81% to 80.34%	31.09% to 57.32%	57.03%	43.75%	Not validated
Overall	19.95% to 80.34%	18.14% to 57.32%	35.12%	28.94%	Validated for low and moderate AOA

In the low to moderate angle of attack (AOA) range, XFLR5 exhibits a reasonable level of agreement with experimental data, indicating its partial validation for design use. Although the deviations from experimental results are higher than those observed for lift coefficients, they remain acceptable for preliminary aerodynamic design.

Overall, the validation analysis shows that XFLR5 provides reasonable drag coefficient predictions in the low to moderate AOA range but lacks accuracy at higher AOA values.

Chapter 4

Design Analysis

4.1 Preliminary Setup for Foil Analysis

The preliminary setup is a crucial step in aerodynamic analysis as it establishes the foundational parameters that significantly influence the accuracy and reliability of the simulation results. Properly defining the flow conditions, such as Reynolds number and flow type, ensures that the analysis closely represents the real-world behavior of the airfoil. Additionally, setting the appropriate air properties and transition modeling techniques directly affects the accuracy of the predicted aerodynamic performance.

Table 4.1: Preliminary Setup for analysis using XFLR5

Parameter	**Value**
Reynolds Number	400,000
Flow Type	Incompressible (Mach 0)
Air Density	1.225 kg/m³
Kinematic Viscosity	1.5e-5 m²/s
Transition Model	e^n Method (NCrit = 7)
Additional Settings	Default

4.2 Xfoil Direct Analysis with the Leading Edge Radius

The leading-edge radius significantly influences an airfoil's low-speed performance and stall behavior. A larger radius typically improves lift at high angles of attack and yields a gentler stall, but can increase drag at lower angles. Using Xfoil Direct Analysis, we can systematically vary the leading-edge radius and quantify its impact on the lift coefficient, drag coefficient, and stall characteristics of the airfoil. The following series of graphs in Figure A.1 presents a detailed visualization of these effects, derived from Xfoil simulations conducted across a range of LER.

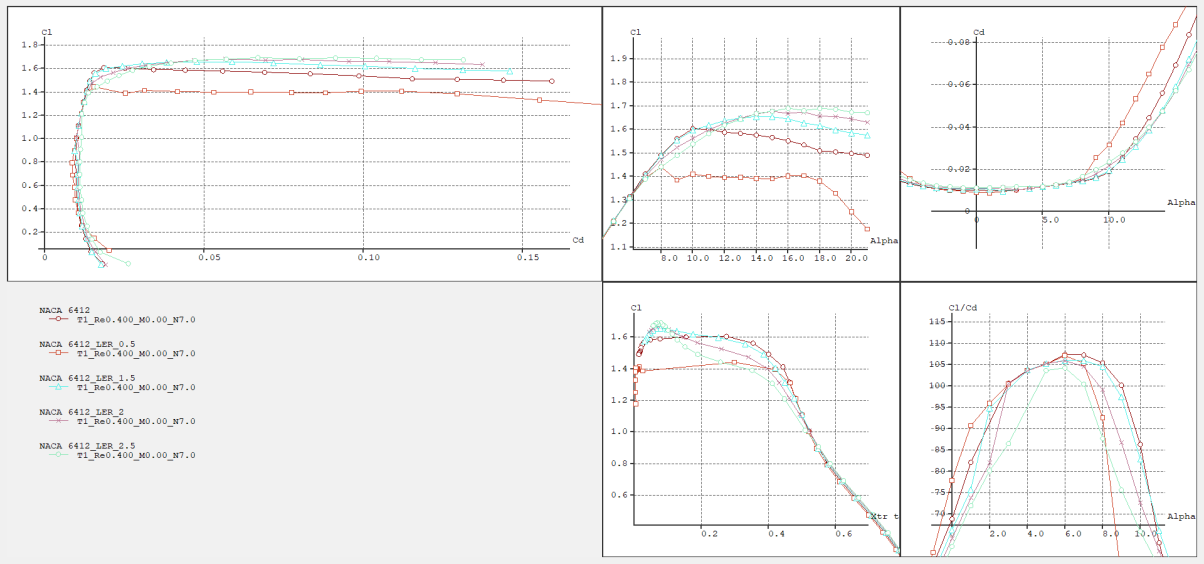

Figure 4.1: Comparative analysis among different values of Leading Edge Radius

Lift Coefficient (CL) vs. Drag Coefficient (CD):

LER ratios of 1.5 and 2.0 demonstrate superior lift-to-drag ratios, particularly in the mid-CD range, compared to the baseline LER 1.0. These higher LER values achieve greater lift with minimal drag increase. LER 0.5 underperforms, exhibiting lower lift and higher drag.

Lift Coefficient (CL) vs. Angle of Attack (alpha):

Increasing LER correlates with improved lift performance. LER values of 1.5, 2.0, and 2.5 generate higher lift across various angles of attack. However, LER 2.5 introduces higher drag, while LER 0.5 demonstrates the poorest performance with lower lift and earlier stall.

Drag Coefficient (CD) vs. Angle of Attack (alpha):

LER 1.5 and 2.0 maintain lower drag across most angles. LER 2.5 exhibits increased drag at higher angles of attack, while LER 0.5 consistently shows the highest drag, indicating the least efficient configuration.

Lift Coefficient (CL) vs. Transition Location (xtr/t):

Higher LER values, notably 1.5 and 2.0, display a more gradual boundary layer transition, promoting extended laminar flow and enhanced lift. LER 2.5 shows a slight tendency for earlier turbulence onset, potentially increasing drag.

Lift-to-Drag Ratio (CL/CD) vs. Angle of Attack (alpha):

LER 1.5 and 2.0 achieve the highest lift-to-drag ratios, particularly at moderate angles of attack, outperforming the baseline LER 1.0. LER 0.5 demonstrates significantly lower efficiency, while LER 2.5 shows a further decrease in aerodynamic efficiency.

4.3 Xfoil Direct Analysis with the Trailing Edge Thickness

While seemingly subtle, trailing-edge thickness plays a crucial role in determining airfoil drag, particularly at lower Reynolds numbers. A thinner trailing edge promotes cleaner flow separation, reducing

pressure drag and improving overall aerodynamic efficiency. Xfoil Direct Analysis allows us to explore the trade-offs between trailing-edge thickness, drag reduction, and potential manufacturing constraints. The accompanying graphs in Figure 4.2 illustrate the impact of varying trailing-edge thickness on the airfoil's drag coefficient and other relevant aerodynamic parameters.

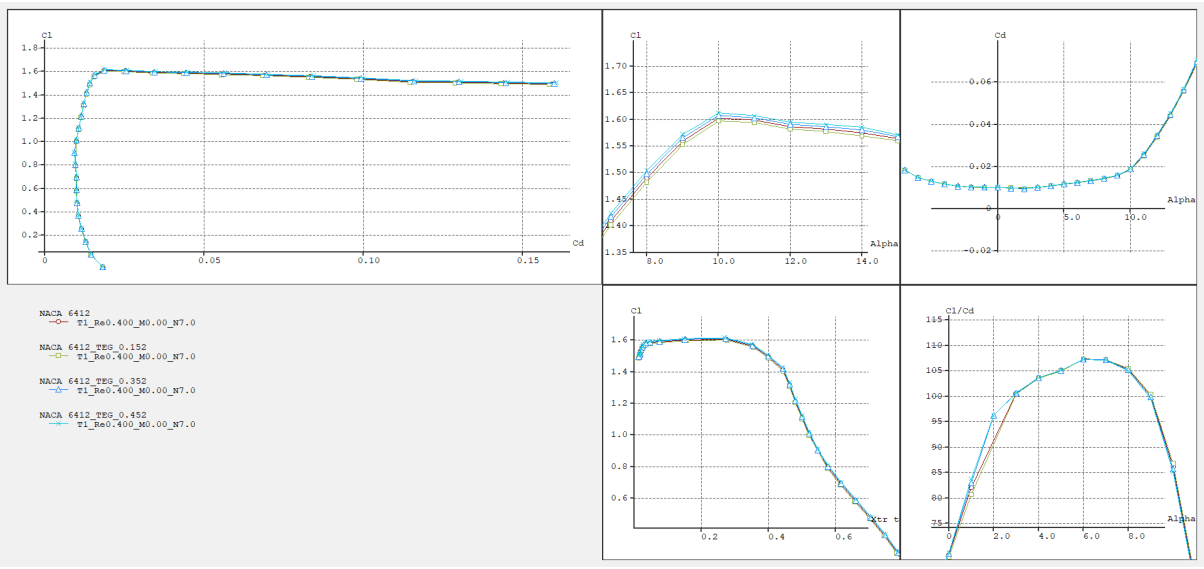

Figure 4.2: Comparative analysis among different values of Trailing Edge Thickness

Lift Coefficient (CL) vs. Drag Coefficient (CD):

All TEG values exhibit similar performance with minor variations. TEG 0.452 emerges as optimal, providing marginally higher lift with minimal drag increase.

Lift Coefficient (CL) vs. Angle of Attack (alpha):

TEG 0.452 consistently yields the highest lift coefficients across various angles of attack, optimizing high-lift scenarios. The baseline TEG 0.252 offers a balanced performance but falls short of TEG 0.452's peak lift.

Drag Coefficient (CD) vs. Angle of Attack (alpha):

TEG 0.452 exhibits slightly higher drag at increased angles of attack, compensated by superior lift performance. Baseline TEG 0.252 demonstrates moderate drag characteristics, balancing lift and drag trade-offs.

Lift Coefficient (CL) vs. Transition Location (xtr/t):

TEG 0.452 promotes earlier boundary layer transition, potentially enhancing stall characteristics and lift performance. Baseline TEG 0.252 presents a more balanced transition profile.

Lift-to-Drag Ratio (CL/CD) vs. Angle of Attack (alpha):

TEG 0.452 demonstrates superior efficiency, maintaining high lift-to-drag ratios across a wide range of angles of attack. While baseline TEG 0.252 offers decent efficiency, it does not match TEG 0.452's performance.

4.4 Xfoil Direct Analysis with the maximum camber

Maximum camber directly influences the airfoil's lift coefficient and pitching moment characteristics. Increasing camber generally increases lift at a given angle of attack but also shifts the pitching moment, potentially impacting stability. Xfoil Direct Analysis enables us to explore the relationship between maximum camber, lift generation, and pitching moment behavior to achieve a desirable aerodynamic balance. The following graphs in Figure 4.3 depict the results of this exploration, showcasing the effects of varying maximum camber on the airfoil's performance.

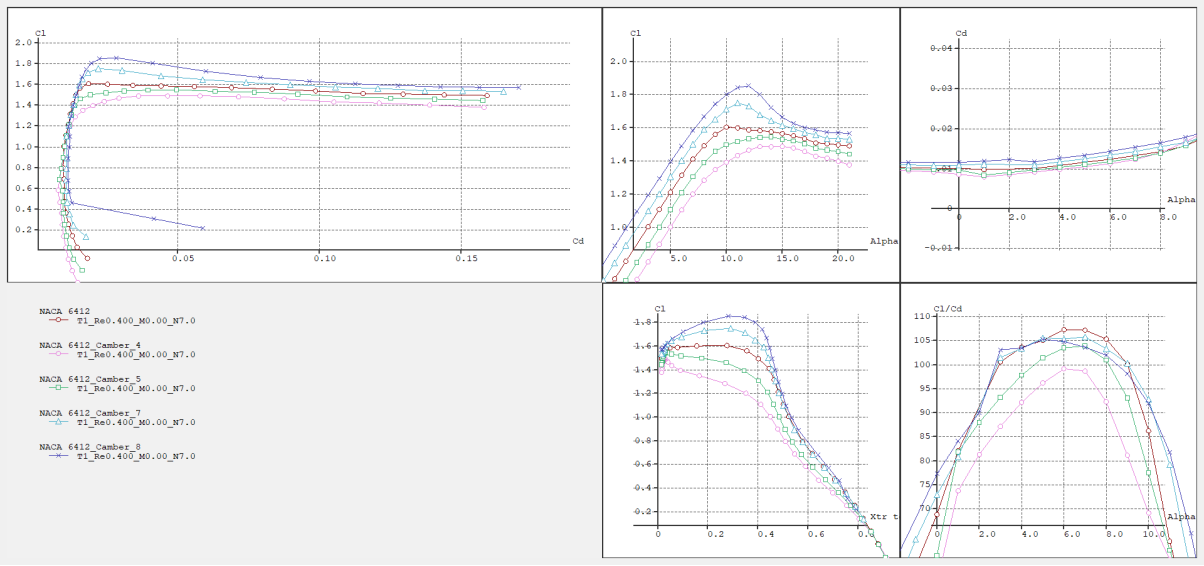

Figure 4.3: Comparative analysis among different values of Maximum Camber

Lift Coefficient (CL) vs. Drag Coefficient (CD):

Increasing camber correlates with higher maximum lift coefficients. The baseline 6% camber demonstrates balanced performance. 8% camber yields the highest maximum lift, albeit with increased drag at lower lift coefficients.

Lift Coefficient (CL) vs. Angle of Attack (alpha):

Higher camber values shift the lift curve upward and leftward. 8% camber generates the highest lift coefficients across most angles of attack, while 4% camber produces the lowest.

Drag Coefficient (CD) vs. Angle of Attack (alpha):

Drag generally increases with camber across most angles of attack. 8% camber exhibits the highest drag, particularly at higher angles, while 4% camber shows the lowest drag at low to moderate angles.

Lift Coefficient (CL) vs. Transition Location (xtr/t):

Higher camber promotes earlier boundary layer transition, especially on the upper surface. 8% camber induces the earliest transition across most lift coefficients, potentially increasing drag but improving stall characteristics.

Lift-to-Drag Ratio (CL/CD) vs. Angle of Attack (alpha):

The baseline 6% camber offers optimal overall L/D performance across a wide range of angles of attack. 7% camber shows a marginally higher peak L/D but over a narrower range.

4.5 Xfoil Direct Analysis with the maximum thickness

Maximum thickness significantly affects both the airfoil's structural properties and its aerodynamic performance. A thicker airfoil can accommodate greater structural loads but may also experience higher drag, especially at higher speeds. Xfoil Direct Analysis allows us to evaluate the aerodynamic trade-offs associated with varying maximum thickness, helping us optimize for both structural integrity and aerodynamic efficiency. A series of graphs is provided in Figure 4.3 to illustrate the impact of maximum thickness variation on key aerodynamic parameters.

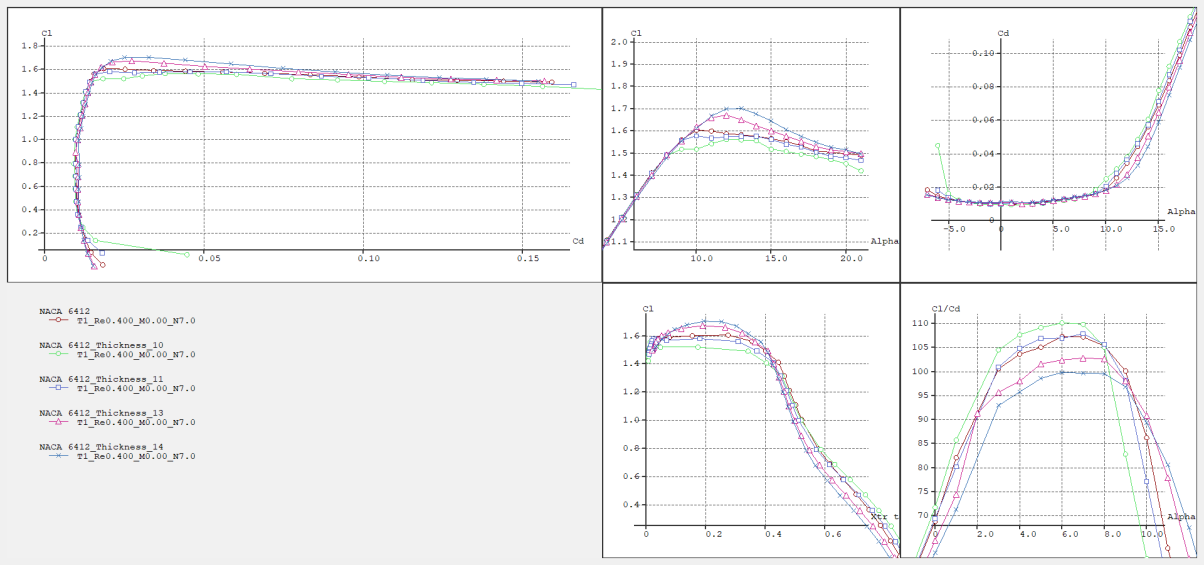

Figure 4.4: Comparative analysis among different values of Maximum Thickness

Lift Coefficient (CL) vs. Drag Coefficient (CD);

Thinner airfoils (10% and 11%) generally produce less drag at lower lift coefficients, while thicker airfoils (13% and 14%) generate slightly higher maximum lift coefficients. The base 12% thickness appears to offer a balanced performance as we can see in the graph.

Lift Coefficient (CL) vs. Angle of Attack (alpha);

Thicker airfoils (13% and 14%) produce higher maximum lift coefficients and maintain lift at higher angles of attack. The 12% base thickness shows intermediate performance, while thinner airfoils have lower maximum lift coefficients but exhibit a more gradual stall behavior.

Drag Coefficient (CD) vs. Angle of Attack (alpha);

Thinner airfoils generally produce less drag at low to moderate angles of attack. However, as the angle of attack increases, the differences in drag become less pronounced among the different thickness values.

Lift Coefficient (CL) vs. Transition Location (xtr/t);

Thicker airfoils tend to have a slightly more forward transition point at lower lift coefficients, which could indicate earlier boundary layer transition. This might explain their slightly higher drag at low lift coefficients.

Lift-to-Drag Ratio (CL/CD) vs. Angle of Attack (alpha);

The 10% thickness airfoil achieves the highest peak lift-to-drag ratio, with the 11% thickness close behind. However, the 13% thickness airfoil demonstrates strong performance across a wide range of angles of attack.

4.6 Design of the Final Airfoil

In this section, we present a comparative analysis between the baseline NACA 6412 airfoil and our final optimized design. The modifications made to the original NACA 6412 profile aim to enhance its performance characteristics, particularly in terms of lift generation and drag reduction. We used XFLR5 software for analysis throughout our design.

4.6.1 Design Insights

These values have been carefully selected to optimize the airfoil's performance, balancing high lift, acceptable drag, and overall efficiency:

- The LEG of 1.5 offers the best balance between lift and drag, providing smooth airflow and high lift at moderate angles of attack. It outperforms LER 1.0 and larger radii like 2.0, maintaining efficiency without structural drawbacks.
- The chosen TEG of 0.452 delivers superior lift with minimal drag increase, particularly at high-lift conditions. The improved boundary layer transition enhances stall characteristics compared to TEG 0.252, making it optimal for varied operations.
- The 6% camber balances lift and drag effectively across a wide range of angles. Higher camber values (7%, 8%) increase drag, while 6% ensures strong overall performance and efficiency.
- The 13% thickness offers a good compromise between structural integrity and aerodynamic efficiency, providing high lift coefficients with reasonable drag characteristics.

Based on the comprehensive analysis of aerodynamic performance, the final design for the NACA 6412 airfoil has been established with the following parameters in Table 4.2:

Table 4.2: Final design parameters for the NACA 6412 airfoil

Parameter	**Value**
Leading Edge Radius (LEG)	1.5
Trailing Edge Gap (TEG)	0.452
Camber	6%
Thickness	13%

Figure 4.5 presents a visual comparison between the baseline NACA 6412 airfoil and our optimized design. The modifications to the original profile are evident. These geometric alterations are strategically implemented to address the aerodynamic performance goals identified in our analysis. The optimized profile maintains the general characteristics of the NACA 6412 while incorporating subtle yet impactful changes that contribute to the performance improvements observed in the subsequent aerodynamic analysis using XFLR5 software.

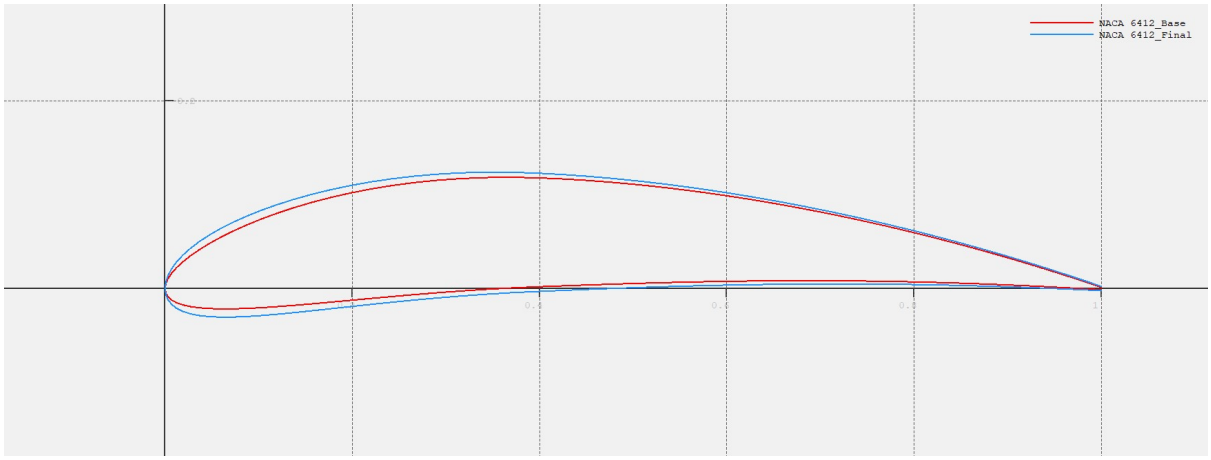

Figure 4.5: Comparison of the base and final design of NACA 6412 airfoil

A newly designed airfoil (blue line) is evaluated against a baseline NACA 6412 airfoil (red line) for application in a Horizontal Axis Wind Turbine (HAWT) operating at a Reynolds number of 400,000. This evaluation, conducted using XFLR5, focuses on key aerodynamic characteristics relevant to HAWT performance. The analyses consider factors such as lift performance, stall behavior, drag characteristics, pitching moment, and aerodynamic efficiency. The results of these performance comparisons are visually represented in a series of graphs provided in Figure 4.6.

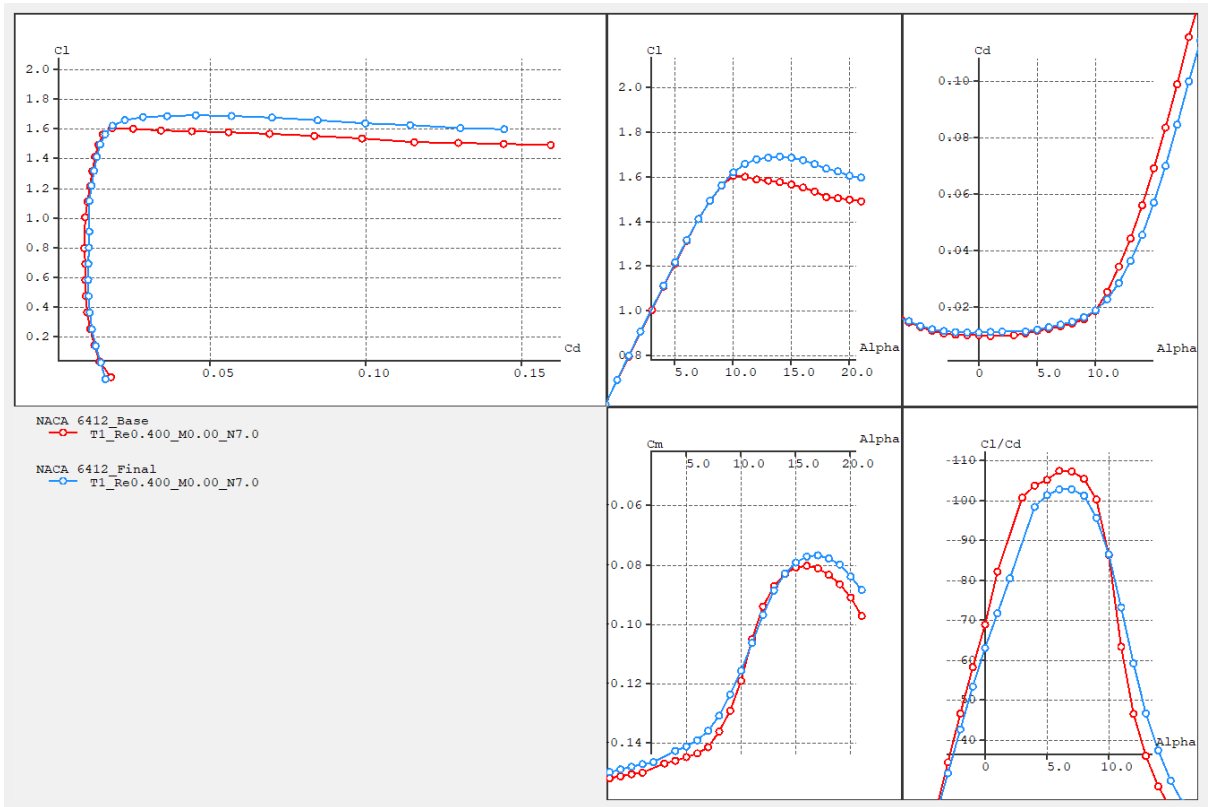

Figure 4.6: Comparative analysis between the base and final design of NACA 6412

The graphs in Figure 4.6 illustrate the following key relationships:

4.6.2 Lift Performance and Stall Behavior

The final design demonstrates a slight increase in maximum lift coefficient (Cl) compared to the baseline NACA 6412 airfoil in C_l vs α graph. This enhancement suggests a potential for improved energy capture at lower wind speeds, a crucial factor for HAWT efficiency. Furthermore, the final design exhibits a marginally higher stall angle of attack, indicating a slightly wider operational range before stall onset. This characteristic could prove beneficial in accommodating varying wind conditions.

4.6.3 Drag Analysis

While the final design shows a slight increase in drag coefficient (Cd) at lower angles of attack in C_l vs C_d graph, typically associated with cruising conditions, it's crucial to note that the drag is actually reduced at moderate to high angles of attack. This drag reduction at higher angles of attack is a significant advantage for HAWT applications. HAWTs often operate at higher angles of attack, particularly at lower wind speeds or during power regulation. The final design's ability to maintain lower drag in these conditions suggests a potential for enhanced efficiency and power output in the operational range most critical for HAWTs.

4.6.4 Pitching Moment and Aerodynamic Efficiency

The final design exhibits a more negative pitching moment coefficient (Cm) across a significant portion of the angle of attack range which can be seen in the C_m vs α graph. This characteristic suggests the potential for reduced structural loads on the HAWT blade, as it might require less downward force from the tail to maintain pitch stability. Regarding aerodynamic efficiency, represented by the lift-to-drag ratio (Cl/Cd), the final design achieves a marginally higher peak value at high angle of attack. While the improvement is modest, it indicates a slight enhancement in overall aerodynamic performance.

4.6.5 Final Verdict

The final optimized design demonstrates several promising characteristics for HAWT application at Re=400,000. The increased maximum lift, higher stall angle, and reduced drag at moderate to high angles of attack suggest the potential for improved power output and efficiency, particularly at lower wind speeds. The more negative pitching moment characteristic could lead to reduced structural loads. While the gain in peak aerodynamic efficiency is marginal, the overall performance improvements, particularly the drag reduction at relevant angles of attack, indicate that the final optimized design is a promising candidate for a HAWT airfoil operating at this Reynolds number.

Chapter 5

Concluding Remarks

5.1 Conclusions

In this project, we designed and optimized an airfoil specifically for Horizontal Axis Wind Turbines (HAWT) operating at a Reynolds number of 400,000, using the NACA 6412 airfoil as the baseline. Through detailed aerodynamic analysis conducted using XFLR5, we aimed to enhance performance by improving lift generation and reducing drag, particularly under varying wind conditions.

5.1.1 Key Findings:

- The final design exhibited a slight increase in maximum lift coefficient and a higher stall angle of attack compared to the baseline airfoil, which is beneficial for energy capture in low-wind scenarios.
- A reduction in drag at moderate to high angles of attack was noted, which is crucial for efficient HAWT performance, particularly during power regulation.
- Improvements in pitching moment stability were observed, potentially leading to reduced structural loads on the turbine blades.
- While enhancements in aerodynamic efficiency were marginal, they still indicate improved overall performance for HAWT applications.

5.1.2 Valuable Lessons Learned

1. **Importance of Aerodynamic Characterization:** Understanding the relationship between lift, drag, and angles of attack was essential for optimizing the airfoil design and improving efficiency for specific operational conditions.
2. **Model Validation:** The significance of validating computational models with experimental data became clear, as discrepancies highlight the limitations of simulation tools like XFLR5.
3. **Iterative Design Process:** The design process reinforced the necessity of iterative testing and modifications, suggesting that even small changes can lead to significant performance enhancements.

5.2 Recommendations

5.2.1 Shortcomings of Design Analysis:

1. **Limited Validation Range:** The validation analysis primarily focused on lower and moderate angles of attack, with less emphasis on higher angles where discrepancies between simulated and experimental data were observed.

2. **Modeling Limitations of XFLR5:** Although XFLR5 is a robust tool for airfoil analysis, it showed limitations in accuracy at higher Reynolds numbers and angles of attack, which could affect the reliability of predictions.

5.2.2 Alternative Approaches for Improvement:

1. **Advanced CFD Simulations:** Utilizing more sophisticated Computational Fluid Dynamics (CFD) tools such as ANSYS Fluent could yield more accurate predictions of aerodynamic performance, especially at higher angles of attack and complex flow conditions.

2. **Experimental Testing:** Conducting wind tunnel tests on scaled prototypes of the designed airfoil would provide empirical data for more thorough validation, potentially revealing insights not captured in simulations.

3. **Consider Alternative Airfoil Profiles:** Exploring other airfoil designs beyond the NACA 6412 and utilizing bio-inspired designs may lead to more innovative solutions that could further enhance lift and drag characteristics.

4. **Iterate Design Based on Real-World Data:** Integrating real-world performance data from installed HAWTs could help refine the design process, ensuring that the airfoil functions optimally across varying operational conditions and environmental factors.

References

[1] H. R. Pratama and M. A. Bramantya, "Numerical studies influence configuration fairing flap track airfoil type naca 4412 and naca 6412 character unmanned aerial vehicle (uav)," in *MATEC Web of Conferences*, vol. 197. EDP Sciences, 2018, p. 08017.

[2] T. Burton, N. Jenkins, D. Sharpe, and E. Bossanyi, *Wind energy handbook*. John Wiley & Sons, 2011.

[3] J. F. Manwell, J. G. McGowan, and A. L. Rogers, *Wind energy explained: theory, design and application*. John Wiley & Sons, 2010.

[4] J. N. Sørensen, "Aerodynamic aspects of wind energy conversion," *Annual Review of Fluid Mechanics*, vol. 43, no. 1, pp. 427–448, 2011.

[5] A. H. A. Hamid, F. Mohamad, M. A. M. Noh, R. E. M. Nasir, and M. A. M. Sapardi, "5. aerodynamics of a modified high-lift low reynolds number airfoil: Preliminary analysis," *International journal emerging technology and advanced engineering*, 2022.

[6] D. H. Le, T. B. Nguyen, and V. M. Ngo, "Experimental performance of a novel dual- stage counter-rotating small wind turbine and forming a validatable cfd computational model," *Energies*, vol. 16, no. 14, p. 5510, 2023.

[7] R. K. Singh, M. R. Ahmed, M. A. Zullah, and Y.-H. Lee, "Design of a low reynolds number airfoil for small horizontal axis wind turbines," *Renewable energy*, vol. 42, pp. 66–76, 2012.

[8] S. J. Miley, "Catalog of low-reynolds-number airfoil data for wind-turbine applications," Rockwell International Corp., Golden, CO (United States). Rocky Flats Plant . . . , Tech. Rep., 1982.

[9] M. S. Selig and J. J. Guglielmo, "High-lift low reynolds number airfoil design," *Journal of aircraft*, vol. 34, no. 1, pp. 72–79, 1997.

[10] D. M. Somers, "Design and experimental results for the s809 airfoil," National Renewable Energy Lab.(NREL), Golden, CO (United States), Tech. Rep., 1997.

[11] Z. Zhang, W. Zhang, Z. J. Zhai, and Q. Y. Chen, "Evaluation of various turbulence models in predicting airflow and turbulence in enclosed environments by cfd: Part 2—comparison with experimental data from literature," *Hvac&R Research*, vol. 13, no. 6, pp. 871–886, 2007.

Appendix A

Important graphs based on the analyses

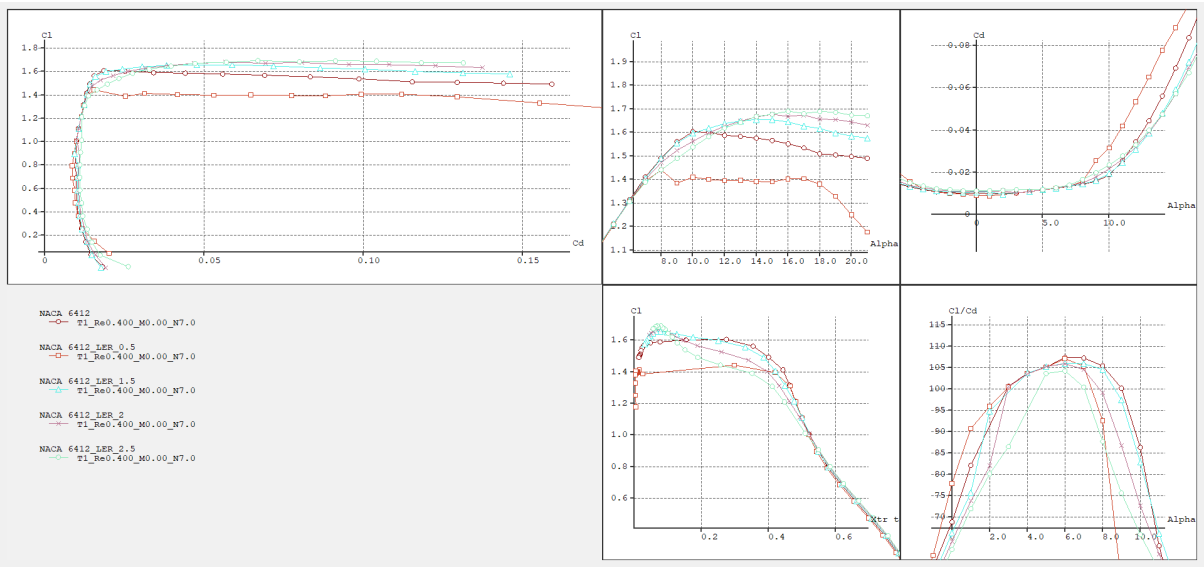

Figure A.1: Comparative analysis among different values of Leading Edge Radius

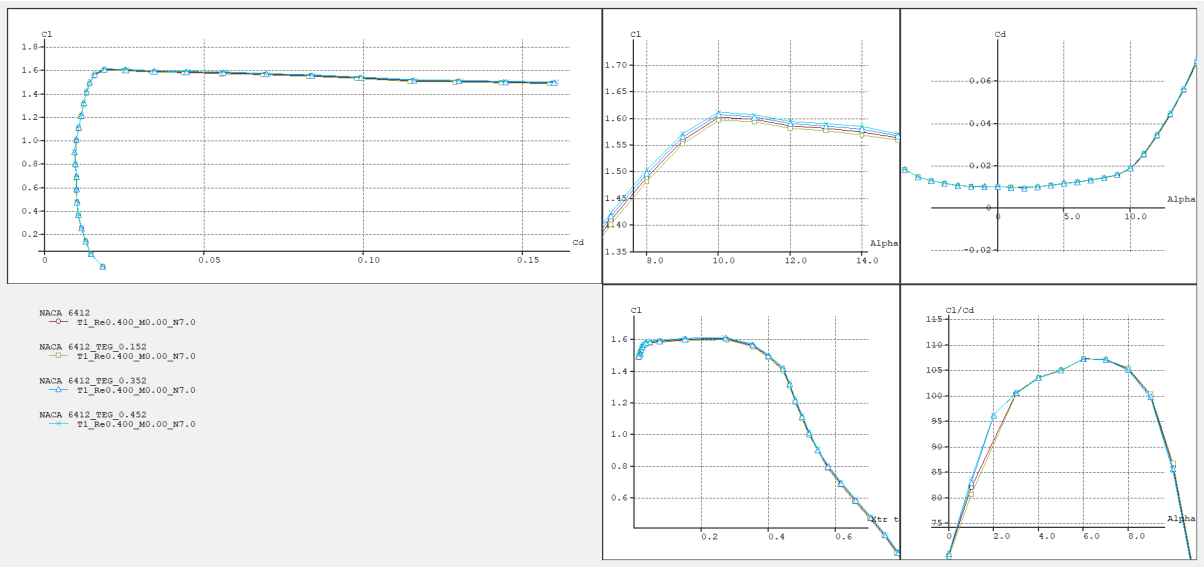

Figure A.2: Comparative analysis among different values of Trailing Edge Thickness

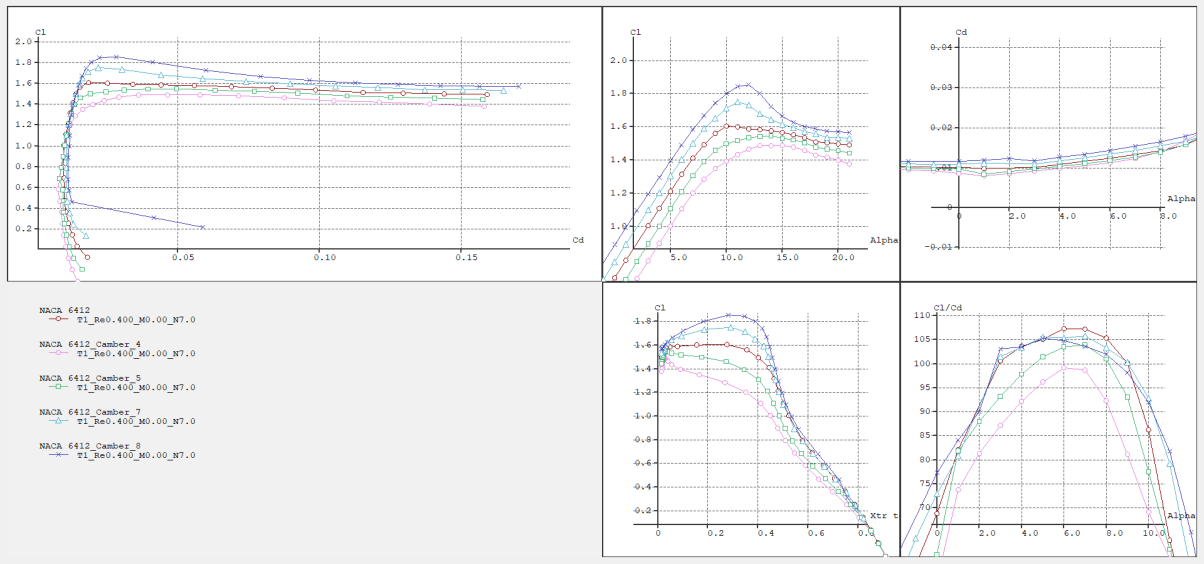

Figure A.3: Comparative analysis among different values of Maximum Camber

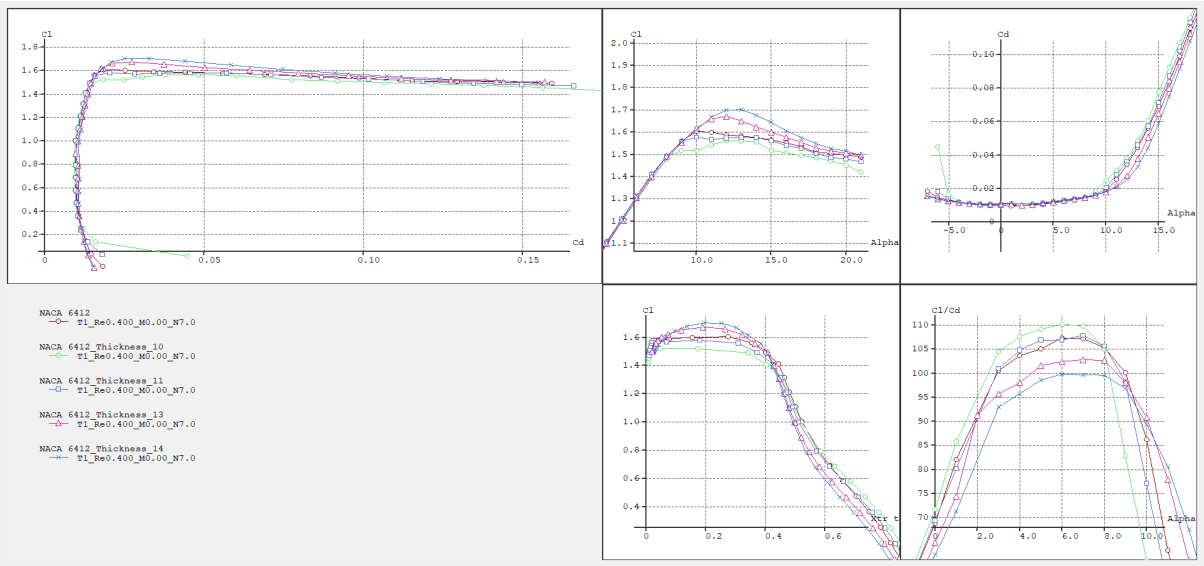

Figure A.4: Comparative analysis among different values of Maximum Thickness